Proceedings of the joint ICVRAM ISUMA UNCERTAINTIES conference
Florianópolis, SC, Brazil, April 8-11, 2018

Strategy for Sensitivity Analysis of DEMO first wall

Dominic C Calleja[1], Wayne Arter[2], Marco De-Angelis[1] and Edoardo Patelli[1]

[1]University of Liverpool, Institute for Risk and Uncertainty,
Chadwick Building, Liverpool, Peach Street, L7 7BD,
email: edoardo.patelli@liverpool.ac.uk
[2]Culham Centre for Fusion Energy, CCFE,
Culham Science Centre, Abingdon OX14 3DB;

Keywords. Nuclear Fusion, PFC, Sensitivity Analysis, Assembly Tolerance

Abstract. Nuclear fusion, the process by which the Sun generates energy, is proposed as one solution to secure the future of global energy supply. If successful it will provide an unlimited source of clean energy. Probably the most promising approach to harnessing fusion for energy production is that of the Tokamak device, a magnetic confinement device of toroidal shape, here enormous magnetic fields are used to contain the 100 m^oC plasma. The first wall blanket of fusion devices (the protective shield on the inside of the reactor vessel) must withstand high heat fluxes, the power handling capabilities of such installations is a significant limiting factor in the future feasibility of thermonuclear fusion for energy production. This study presents a computational methodology for the evaluation of such designs in the presence of uncertainty in assembly tolerance. Methods for the analysis of first wall installations are outlined, including an initial Monte Carlo study of the first wall to develop understanding of the complex effects of tile misalignment. Approaches to local and global sensitivity analysis in order to rank the effects of particular dimensions of displacements, and the use of parallel coordinate plots to develop an intuitive method to visual sensitivity analysis in high dimensional domains.

1 INTRODUCTION

DEMO (DEMOnstration Power Station) represents the final step in development before commercial fusion. DEMO aims to build on the the ITER experimental reactor, currently under construction, intended to prove fusion as a viable source of clean energy. DEMO should produce and harvest electrical energy on the scale of modern conventional electric power stations. The US, EU, Russia, Japan and other partners within the World Fusion Programs are engaged in the preliminary design phase of DEMO devices. It is likely that a number of these will be constructed world wide [1].

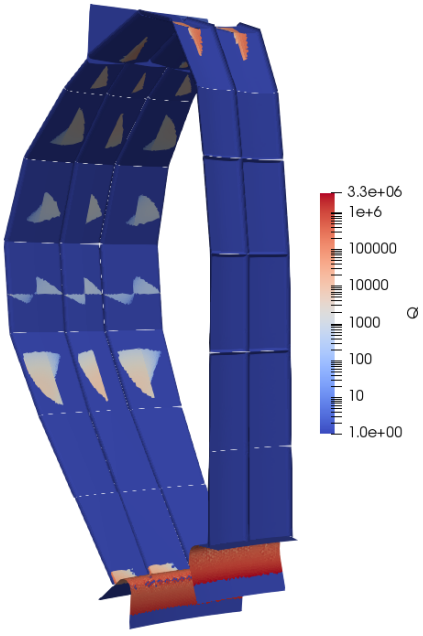

Figure 1: Visualisation of typical flux distributions for ideal outboard DEMO geometry generated with SMARRDA

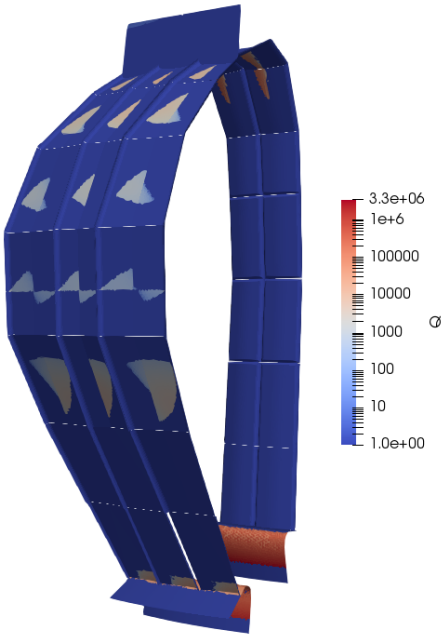

Figure 2: Visualisation of typical flux distributions for ideal inboard DEMO geometry generated with SMARRDA

In the DEMO device the first wall components are exposed to charged particle heat loads, fast particle loads, radiative loads, and heat loads from disruption events. All contribute to the overall load on Plasma Facing Components (PFCs). This study focuses on the effects of particle loading. In particular, it is this phenomenon dominating the geometry and assembly of such installations, relating to the propagation of such particles along magnetic field lines within the vessel. The power handling capabilities of PFCs depend on both their design and precision of assembly. In devices such as ITER and JET, tiles (constituent components of the first wall) exhibit complex shapes, one consideration in this endeavour is to maximize power load performance whilst allowing for some degree of misalignment [12].

Challenges relating to the first wall power handling are significantly higher in DEMO than ITER. A first review of loads pertaining to DEMO has been conducted, based on initial rather crude designs, projected loads of $7MW/m^2$ have been calculated [14]. This study highlights the considerable space for design optimization and further assessment of DEMO first wall technologies. Preliminary load design limits for DEMO during steady state operation are presumed to be not higher than $1.0MW/m^2$, considerably lower than those expected for ITER.

This lower requirement is due to the need for DEMO to incorporate (1) tritium breeding, necessitating higher neutron absorption, (2) higher coolant temperatures for efficient power conversion, (3) materials able to withstand high neutron fluency and significant radiation damage with low activation [6]. DEMO will require significant advances on current fusion technologies, DEMO is bigger, more powerful, and will need to have operation times orders of magnitude greater than any devices available today. Whilst ITER aims to tackle a number of technological challenges of better plasma confinement, longer pulse duration, sustaining D-T operation, testing tritium breeding, and much higher fusion power gain than the current record; DEMO will be the first to attempt to harvest fusion power, the first wall will be essential in this endeavour. Therefore effective tools to understand and manage the uncertainties in the development of these future devices will be essential to their success.

Efforts to understand and manage uncertainties relating to the first wall challenge could identify significant opportunities on the path to fusion for energy production. ITER is an excellent example of the cost and complexity of developing future fusion technologies, running behind schedule and over budget. Uncertainty quantification could help identify and navigate potential delays in the DEMO development. For example, study of the uncertainties relating to the first wall may identify opportunities to increase the tolerance limits in the assembly, this would have a real and tangible saving to the future DEMO budget. Assembly uncertainty studies could identify high priority regions of the vessel where certain tile misalignments could have a critical effect on the reliability of PFCs, identifying these risks to design engineers long before critical system failure, or providing mitigation opportunities to build in resilience.

2 SOFTWARE

Two software packages have been utilized in this study, SMARRDA to calculate the predicted heat flux on PFCs, and the OpenCossan package for uncertainty quantification.

2.1 SMARDDA

SMARDDA is a software library to model plasma interaction with complex engineered surfaces. The simple flux-tube model of power deposition allows for the following of field lines until intersection with CAD geometry. Recent advancements to the code aid rapid/efficient power decomposition predictions for PFCs, even with complex geometries. The relative efficiency of the code allows for its use in numerical analysis of uncertainty. With incorporated modules for geometry manipulation, the software suit lends itself to a study of first wall assembly tolerance.

SMARDDA is a package originally developed in 2007/08 by UKAEA, and is a collection of object-orientated Fortran-95 modules for ray, particle and fieldline tracing. Originally used for modelling the interaction of neutral particle beams with the low temperature gas found in neutral beam ducts [4]. The wider context of the development was in response to the need to heat high temperature plasma's in magnetic confinement devices. This has since been extended to modelling of charged particles interaction with CAD geometry in magnetic fields, such as those found in magnetic confinement devices. A detailed description of constituent codes, and basis of the flux-tube model for modelling power deposition in tokamak edges can be found [3].

2.2 COSSAN

Cossan is a general purpose software package for uncertainty quantification and management, sensitivity, optimization, reliability analysis and robust design. The package is designed to provide even the novice with access to the most cutting edge algorithms for uncertainty quantification, and seamless interaction with any third party solvers (such as in this case SMARDDA)[9][10][11]. Two versions of the package are currently available, OpenCossan and Cossan-X. The former developed in the object-orientated MATLAB environment and is available under GNU LGPL licence. The latter is a commercially licensed GUI version of the OpenCossan engine, providing a user-friendly graphical environment for the rational quantification and propagation of uncertainties. With parallel computing features, and ability to develop bespoke work flows, COSSAN provides a solution to the cost and complexity of stochastic analysis.

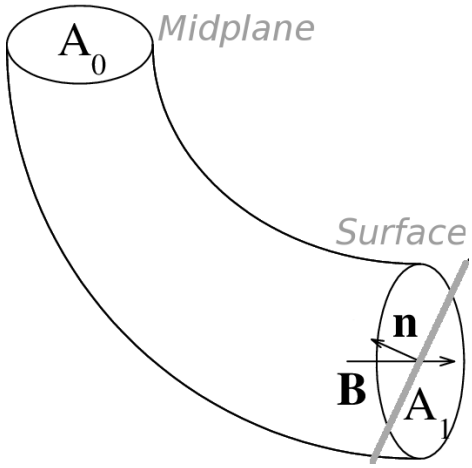

Figure 3: Flux tube model for field, **B** from mid plane (plasma) to PFC surface (on tile) [3]

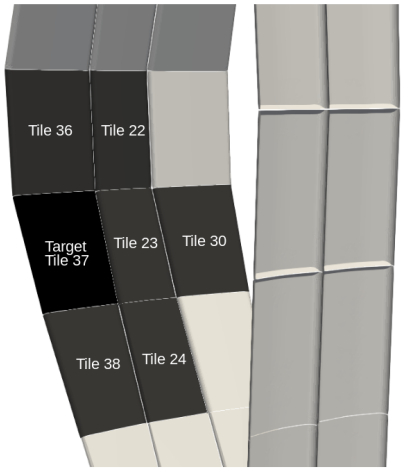

Figure 4: Target tile and adjacent bodies used in sensitivity case study

3 MODELLING FIRST WALL OF FUSION DEVICES

The DEMO first wall geometry is based on 18 fold toroidal symmetry, with each toroidal segment consisting of 38 individual tiles. With a major radius in the order of $9m$ modules are expected to have frontal areas in the order of $1:2m$, providing some indication of the sensitivity of the tiles performance to assembly tolerance, as relativity small displacements can expose large surfaces to dangerous fluxes locally. The initial European DEMO wall design is used with plasma configuration parameters for the flat-top phase, x-point discharge, and a scrape-off layer power fall off length (λ_q) of $0.05m$. With these being the current best estimates for the configuration where DEMO is likely to spend most of its in operation time.

3.1 Power Deposition

As alluded to, particle loading dominates in the design of the first wall. Both neutron and ion bombardment of PFCs are indicative of Deuterium Tritium (D-T) operation regimes in DEMO. The neutron path is undisturbed by the magnetic field. Typical ion gyro-radius is very small, in the order of μm, whilst plasma minor and major radius is in the order of m, hence it is appropriate to approximate ion path to follow field lines. In order to distribute the power over as large a possible area it is necessary to design PFCs such that field lines intersect surface at close to tangential incidence. It can be seen that as the field $(\mathbf{B})$ tends to the perpendicular of surface normal $(\mathbf{n})$, power (Q) tends to zero.

$$Q = C_{std}\mathbf{B}\cdot\mathbf{n}\exp\left(-\frac{(\varphi-\varphi_m)}{(\lambda_m R_m B_{pm})}\right) \tag{1}$$

Where, λ_m governs the rate of decay of power from the last closed flux surface in the scrape off layer. The values of flux function φ, and φ_m at the mid plane, and poloidal flux at geometry plasma intersection respectively. C_{std} is the derived power normalization factor for given equilibrium and geometry [3].

3.2 Tile Misalignment

Under the assumption that ion's propagate along magnetic field lines (disregarding collective turbulence), the high heat fluxes found in the scrape off layer of a Tokamak device are attenuated by acute angles of incidence between tile surface and magnetic field lines. The strong toroidal component of the field makes it possible to typically achieve incidence angles of between $1-5^o$ for the majority of the front face of PFCs. However, at tile intersection gaps, and along the exposed edges of any ducts into the chamber, far larger angles are ineviTable, even with complex chamfers and edge shaping $15-90^o$ [7].

Whilst higher flux at tile edges can be mitigated in the design of first wall modules, unintentional misalignment can significantly exacerbate the risks. There are a number of potential causes for misalignment's to occur, from issues with initial assembly, disruption induced loading, thermal expansion, or deformation from continued loading in the $>5T$ magnetic fields.

The impact associated with edge localized heating in the first wall cannot be understated. High surface temperatures at the edges of tiles increases the risk of material evaporation and sputtering, with the potential of plasma contamination, these impurities have significant effect on plasma operation [7]. Component life can also be heavily impacted, an increased concern with DEMO, as in operation time will need to be in the order of months or years to prove economic viability. DEMO will also require an actively cooled first wall, for both energy production and to sustain longer pulse duration. Localized heating could cause large thermal gradients, and increased differential expansion leading to substrate

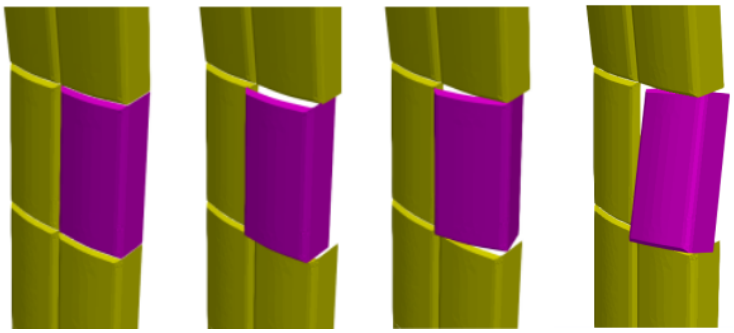

Figure 5: Dimensions of displacement considered in the sensitivity analysis of DEMO first wall, [no displacement, displaced normal to tile surface, rotated about toroidal axis, and the poloidal axis of the tile]

delamination between the cooling installation and tile surface material.

4 UNCERTAINTY QUANTIFICATION

A computational approach to the sensitivity analysis of the first wall in the presence of uncertainties due to ineviTable assembly tolerances is presented. Results for an initial input domain exploration are presented along with some initial conclusions. A methodology for the detailed examination of a tile is also outlined for a single tile test case. Included in this process is a study of the tile given small perturbations from the ideal case, possibly misalignments of the magnitude that are highly likely inside an operational DEMO device. A parameterised sensitivity study of the feasible tolerance domain for the local region of the vessel is also conducted, the definition of the local region of the vacuum vessel can be found in fig. 4. Finally parallel coordinate plots are presented for the test case which can aid in the visualization of high dimensional data, with a more intuitive approach to visual sensitivity studies.

4.1 Input domain exploration

Given 38 modules in each toroidal segment, each having 3 dimensions of displacement, and significant higher order interactions, an initial input domain exploration has been conducted. A Latin Hypercube Sampling (LHS) regime has been employed. With the high dimensionality of the input domain, the stratified approach to exploration allows one to improve the exploration with fewer model evaluations than a purely random sample, given a relatively computationally expensive finite element model this is helpful. However shadowing by nature is heavily discontinuous, edges can become suddenly exposed, hence there is some concern over the use of LHS. Efforts should be made to investigate any coupling as a result of the discontinuous problem and low discrepancy sampling, to asses the appropriateness of the method. Definitions of the input factors can be found in fig. 5 and the distributions assigned in Table 1.

A review of the results of the LHS investigation in fig. 6 begins to identify some interesting features of the sensitivities of this particular geometry and plasma configuration to tile misalignment uncertainties. Tiles $4:7$ and $12:15$, corresponding to the tiles around the plasma mid plane on the inboard of the geometry show no power deposition. The flux distribution across the surface for these bodies, for the ideal baseline case can be seen in fig. 2, and experience no change in this for any design of experiment (DOE). This would suggest that certainly in the flat-top phase this is a sub-critical region, and could possibly be a candidate for relaxing the limits on the assembly and manufacture tolerance in this region.

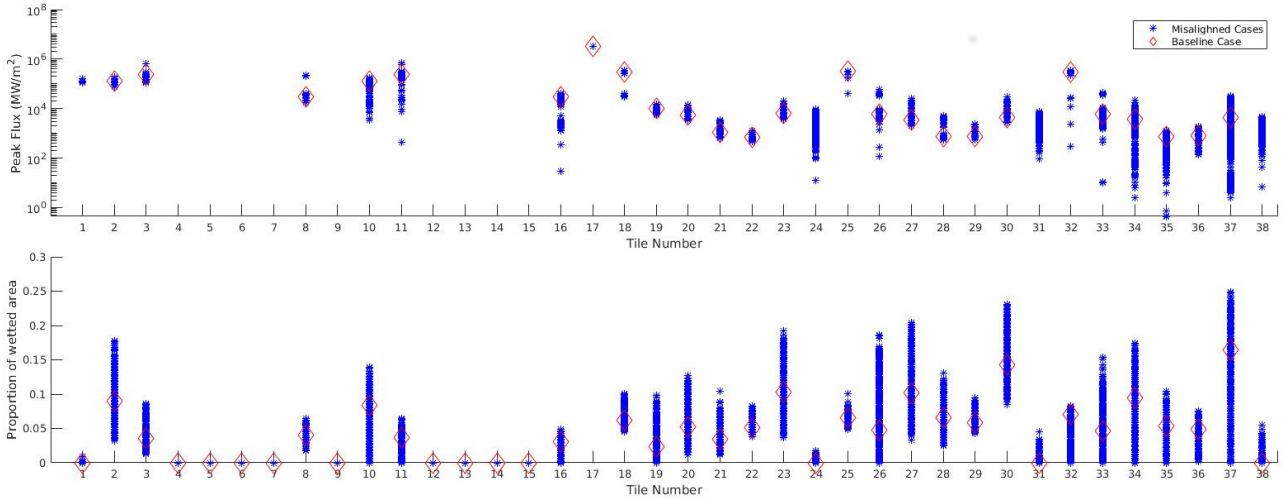

Figure 6: Top : Maximum peak flux for each module, Bottom : proportional wetted area from LHS-MC analysis 8000 samples

Table 1: Displacement input distributions for each of the 37 tiles in the DEMO toroidal segment (Divertor excluded)

Displacement	Distribution	Distribution Limits	Units
Normal to Tile Surface	$N(0,3.5)$	[-20,10]	cm
Tile Toroidal axis	$N(0,0.8)$	[-1.5,1.5]	^{o}
Tile Poloidal axis	$N(0,0.8)$	[-1.5,1.5]	^{o}

The results of some tiles in fig. 6, highlight the discontinuous nature of the shadowing previously alluded to. Observing the peak flux values for tile 26, shows 4 distinct groupings to the peak flux values recorded, a phenomenon repeated by a number of other tiles. This discontinuity is very likely due to the sudden exposure of edges with much higher incidence angles of the fieldlines at these edges, than the tile front surface. The same trends are not as prominent in the proportion of wetted area, suggesting that these peak values are heavily localized, offering further evidence of the edge exposure. These features in the data can be observed for at least 11 of the tiles, suggesting edge localized loading of the tile as a result of misalignment is of concern in a number of regions of the vacuum vessel. This analysis should be repeated for a purely random sample also to estimate any influence of the stratified sampling regime.

Interrogation of fig. 6 allows for an initial selection of a tile for further analysis. Given the large variation in both proportion of wetted surface and peak flux, module 37 has been selected. What follows is a detailed investigation of this particular body, a similar process can be replicated for any and all modules.

4.2 Local Sensitivity analysis

Given all DEMO devices will be precision engineered installations it is appropriate to first investigate small perturbations around the ideal case, with these being the most likely. Local sensitivity analysis is the assessment of the local impact of input factors variation on model response by concentrating on the sensitivity in vicinity of a reference point, the reference point in this case being the ideal design.

The method of local sensitivity by Monte Carlo has been employed, available in the COSSAN sensitivity toolbox. This method estimates the relative importance of input factors by means of the Monte Carlo method [8]. The method first uses small perturbations in the input domain (j random samples) around some reference point $\tilde{x}$ (in this case the idea design), to estimate the gradient of a generic function $g(x)$ in this local region. Each input parameter k is perturbed independently $x_k^{(j)} = \tilde{x}_k + \gamma \cdot r_k^{(j)}$ where $r^{(j)}$ is a random vector. Hence the components of the derivative are,

$$d_i(\tilde{x}) = \frac{\partial g(x)}{\partial x_k}\bigg|_{x=\tilde{x}} \lim_{\gamma \to 0} \frac{g(\tilde{x}_1,...,\tilde{x}_k + \gamma r_k^{(j)},...,\tilde{x}_n) - g(\tilde{x})}{\gamma r_k^{(j)}} \tag{2}$$

Since the variation $\gamma r_k^{(j)}$ are assumed to be very small,

$$d_i(\tilde{x}) \approx \frac{g(\tilde{x}_1,...,\tilde{x}_k + \gamma r_k^{(j)},...,\tilde{x}_n) - g(\tilde{x})}{\gamma r_k^{(j)}} = \frac{\partial g(x)}{\partial x_k} \tag{3}$$

The local relative importance measure of each parameter $S_i(x_k)$ is then,

$$S_i(x_k) = \frac{\sigma_k}{\sigma_Y} \left| \frac{\partial g(x)}{\partial x_k} \right|_{\tilde{x}} \tag{4}$$

Where, σ_k and σ_Y are the standard deviation of the input factor k and output Y. The relative importance of each input factor, for tile 37 and all adjacent tiles is found in fig. 7.

The local sensitivity has been conducted with input factors of 3 dimensions of misalignment for tile 37 and all adjacent bodies, displayed on the horizontal axis of fig. 7, with following number corresponding to the tile number being displaced, maximum flux on the target tile is the metric used for the analysis. The Monte Carlo approach to local sensitivity analysis performs very well in high dimensional space, requiring few model evaluations. As was expected the vast majority of input dimensions have no effect on the peak flux of tile 37. The most important inputs are those of the target tile, with minimal impact from the displacement of adjacent bodies, fig. 7. Small perturbations from the ideal design minimizes the potential of adjacent tiles displacements exposing significant surface areas of the target, correspondingly no significant increase in wetted area of the tile is identified in such instances. Whilst small perturbations of the target can increase the angle of field line incidence with tile surface, hence increasing peak flux.

fig. 8 shows the heat flux distribution of the target tile for the baseline case, $1mm$ radial displacement away from the plasma, and $1mm$ radial displacement toward the plasma (negative convention for SMARRDA). Given the small displacements a significant effect can be observed for the proportion of wetted area on the surface of the tile, less clear from the visualization is the increase in maximum flux value for the tile surface of $1.2E-4MWm^{-2}$, or a penalty factor

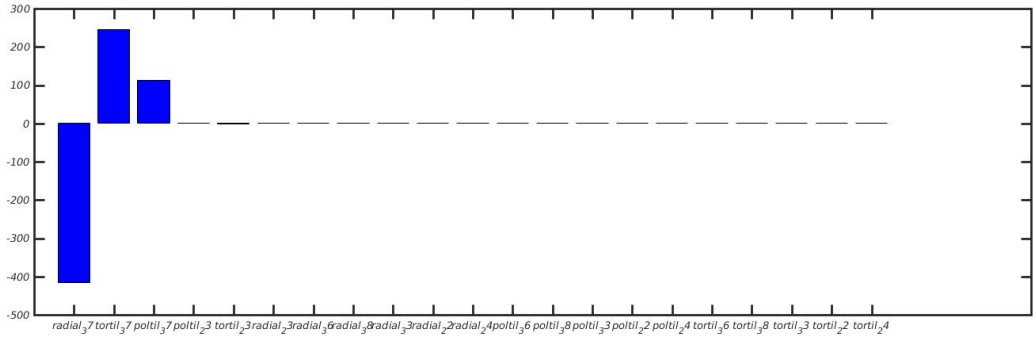

Figure 7: Local sensitivity analysis, relative importance for tile 37, adjacent tiles inputs displayed

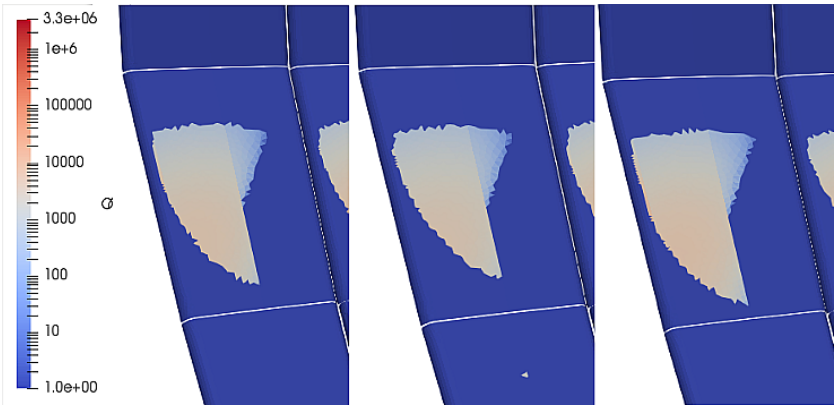

Figure 8: Heat flux distribution for the 'target' tile (tile 37) Left : Ideal baseline case, Centre : $+1mm$ displacement from the ideal case radially (away from the plasma), Right : $-1mm$ displacement from the ideal case radially (toward from the plasma)

of 2.8%. This in conjunction with a similar process for the toroidal and poloidal displacement cases confirms the results of the local sensitivity study in fig. 7, with these two displacements having a smaller impact on the peak flux. With Tile dimensions in the order of meters, observing significant cost to relatively small displacements further identifies the challenge of the first wall assembly in fusion devices, and the need to optimize the tile shaping for some degree of misalignment, there are significant gains to be made where these tolerance limits can be relaxed.

4.3 Global Sensitivity Analysis

Given the computational effort in evaluating the model it is necessary to employ a method for global sensitivity analysis which reduces the required number of model evaluations. The random balanced design methodology is one such approach. N design points are selected over one curve in the input space, at frequency of 1 for each factor, covering a subset of the input domain. Random permutations of the coordinates of these design points are then taken in order to cover the whole input space, and the model is evaluated at each design point. A Fourier spectrum is then calculated for the model outputs at frequency of 1 and its higher harmonics, yielding estimates of the sensitivity index for all inputs. This method provides estimation of the main effects for each uncertain input, it is effective in high dimensional space and for non-linear and non additive models [13] [5].

The global sensitivity analysis has been conducted for the local region of the vacuum vessel, the target tile and those adjacent to it, fig. 4, similarly to the local analysis maximum flux is the metric used also for the global. The global sensitivity analysis is concordant with the results of the local, identifying the displacements of the target tiles as contributing most to the variance on the maximum flux value for tile 37, when the whole input domain is considered. However the toroidal rotation now dominates, with the poloidal second, as opposed to the radial. fig. 10 shows the heat flux for the target tile for the ideal case, upper and lower bound of the applied distribution for the toroidal rotation from Table 1. In the centre plot significant edge localized loading can be observed from the applied displacement, the additional risks this presents for the first wall performance are profound [2]. Additionally the right visualization in fig. 10 shows a predicted case of total shadowing of the tile front surface, a major concern for future DEMO devices as it is likely the energy harvesting will rely on the active cooling of the modules [6], so efficient operation will require maximizing the wetted area.

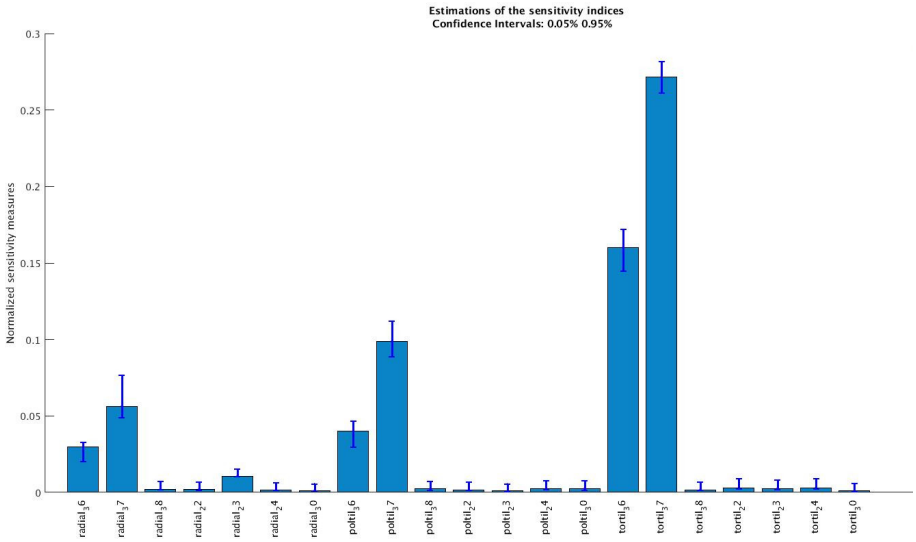

Figure 9: Global sensitivity indices for possible displacements of tile 37 and all adjacent tiles using the RBD method

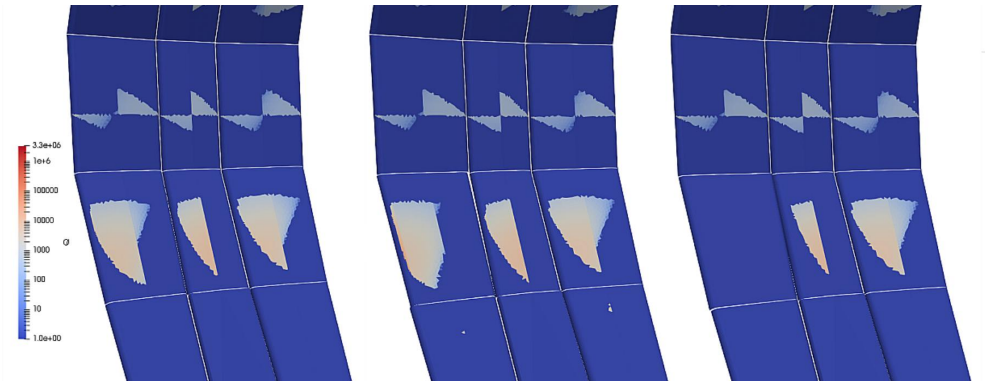

Figure 10: Heat flux distribution for the 'target' tile Left : Ideal baseline case, Centre : $+1.5^o$ rotation about the toroidal tile axis, Right : -1.5^o rotation about the toroidal tile axis

4.4 Parallel Coordinate Analysis

Parallel coordinate plots provide a convenient way of visualizing high dimensional data. In this case the parallel coordinate view provides an approach to interrogating the results, and an informative visual sensitivity analysis. The parallel coordinate plot in fig. 11 has been generated from the results of the previously discussed LHS Monte Carlo, so has required no further computation. In order to produce the plot all inputs have been re-scaled to between 0 and 1, along with the output *MaxQ* for tile 37. Each line on the upper plot represents a single model evaluation, with the normalized value of each random input and the normalised output, maximum flux for the target. The data has been further discretized into five quantile groups based on the output. The lower plot in fig. 11 is displaying the median value of each discretized group, for each input and the output.

Some interesting features arise from such an analysis. Primarily this acts as a validation of the global sensitivity analysis in fig. 9. Where the min and max quantile group medians deviate furthest from one another, this gives strong indication that this factor is heavily contributing to the variance in the output. As the maximum group tends toward 1 the output tends to increase suggesting this displacement is contributing to an increase in flux for the tile, the inverse is also true. Similarly to the global sensitivity results the tortil, poltil and radial (or normal to tile surface) inputs for the target show the greatest divergence between the upper and lower discretized set. Examination of the flux distribution on the target tile under such conditions validate this conclusion, fig. 10 shows a comparison of flux distributions on the target tile between the ideal case, and the upper and lower bounds $[1.5, -1.5]^o$ of toroidal rotation of the tile 37. The bottom plot in fig. 11 similarly indicates that the greatest divergence between the median of the minimum and maximum quantile groups of the output is caused by the toroidal tilt of tile 37. Therefore it is likely that those DOEs that have predicted the highest flux will include samples from the upper range of the input variable tortil 37.Comparison of the flux maps in fig. 10 show agreement, as the toroidal rotation in one direction gives predictions of total surface shadowing, and in the opposite direction increases in both the wetted area and peak flux value.

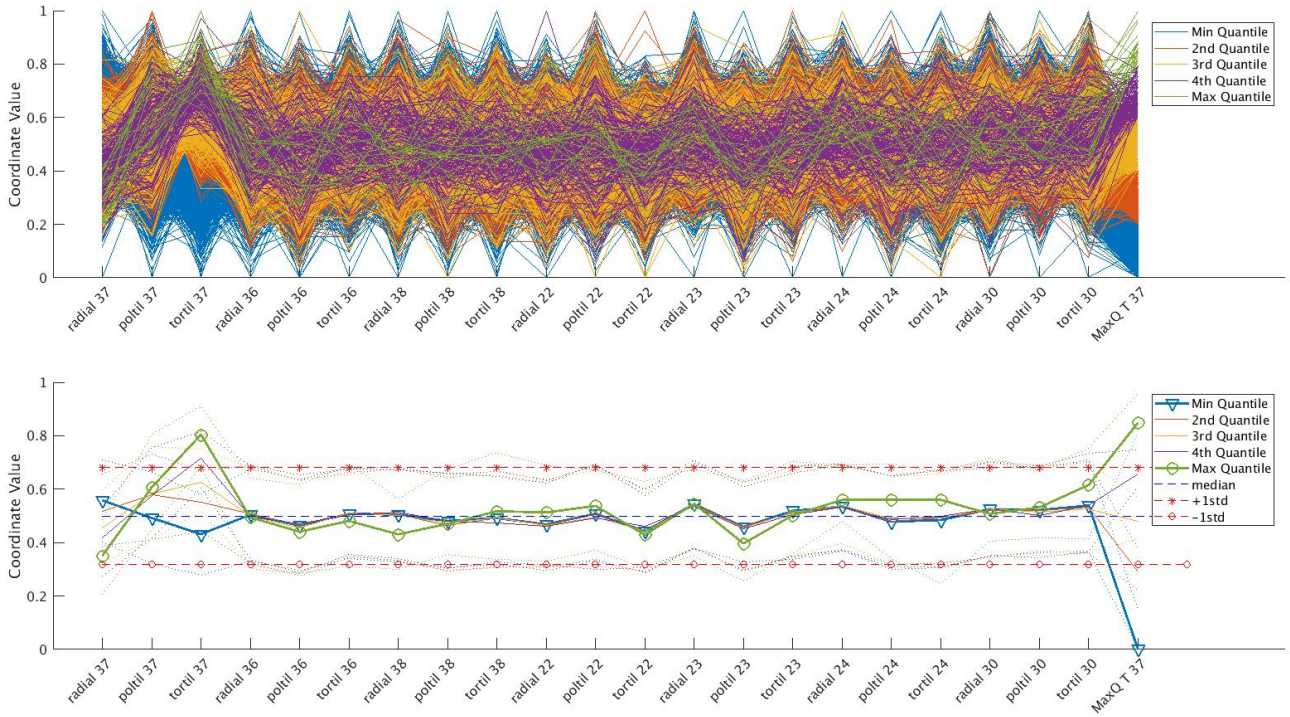

Figure 11: Top : Parallel coordinate plot of normalized displacements and discretized output. Bottom : parallel coordinate plot median of each discretized subset

5 CONCLUSION

This study presents some initial work in the examination of assembly uncertainties for the first wall of the DEMO generation of thermonuclear devices. Whilst this study has focused on one particular tile a similar approach can be conducted for all tiles and modules of the first wall, and indeed this should be conducted, as each region of the vacuum vessel is unique. Future work will include the refinement of the proposed approach and application to all modules within the toroidal section. This analysis has been restricted to one of the 18 fold symmetrical segments of the DEMO first wall, and initial indication of the impact of adjacent tile displacements is clear. This presents further opportunities to examine larger arrays of tiles in order to examine a larger potential footprint, particularly in limiter configuration cases. Further to this, the outboard portion of the geometry in practice will likely be designed in modules (each module consisting of 3 tiles) examining these modules as a unit will also be of significant interest to reactor designers.

ACKNOWLEDGEMENTS

This work has been supported by the EPSRC-ESRC Centre for Doctoral Training on Quantification and Management of Risk & Uncertainty in Complex Systems & Environments Grant number (EP/L015927/1)

Additionally this work has been carried out within the framework of the European Fusion Agreement. The views and opinions expressed herein do not necessarily reflect those of the European Commission.

REFERENCES

[1] Mohamed Abdou et al. “Blanket / first wall challenges and required R & D on the pathway to DEMO”. In: *Fusion Engineering and Design* 100 (2015), pp. 2–43. ISSN: 0920-3796. DOI: 10.1016/j.fusengdes.2015.07.021. URL: http://dx.doi.org/10.1016/j.fusengdes.2015.07.021.

[2] G Arnoux et al. “Power handling of the JET ITER-like wall”. In: *Physica Scripta*. Vol. T159. 12. 2014. DOI: 10.1088/0031-8949/2014/T159/014009.

[3] Wayne Arter, Valeria Riccardo, and Geoff Fishpool. “Power Deposition on Tokamak Plasma-Facing Components”. In: (2014), pp. 1–12. DOI: 10.1109/TPS.2014.2320904. arXiv: 1403.7142. URL: http://arxiv.org/abs/1403.7142%7B%5C%%7D0Ahttp://dx.doi.org/10.1109/TPS.2014.2320904.

[4] Wayne Arter, Elizabeth Surrey, and Damian B. King. “The SMARDDA Approach to Ray Tracing and Particle Tracking”. In: *IEEE Transactions on Plasma Science* 43.9 (2015), pp. 3323–3331. ISSN: 00933813. DOI: 10.1109/TPS.2015.2458897. arXiv: arXiv:1403.6750v1.

[5] Emanuele Borgonovo and Elmar Plischke. “Sensitivity analysis: A review of recent advances”. In: *European Journal of Operational Research* 248.3 (2016), pp. 869–887. ISSN: 03772217. DOI: 10.1016/j.ejor.2015.06.032InvitedReview. URL: http://dx.doi.org/10.1016/j.ejor.2015.06.032.

[6] G. Federici et al. “Overview of EU DEMO design and R&D activities”. In: *Fusion Engineering and Design* 89.7-8 (2014), pp. 882–889. ISSN: 09203796. DOI: 10.1016/j.fusengdes.2014.01.070. URL: http://dx.doi.org/10.1016/j.fusengdes.2014.01.070.

[7] R. Mitteau et al. “Allowable heat load on the edge of the ITER first wall panel beryllium flat tiles”. In: *Nuclear Materials and Energy* 12 (2016), pp. 1067–1070. ISSN: 23521791. DOI: 10.1016/j.nme.2017.02.001. URL: https://doi.org/10.1016/j.nme.2017.02.001.

[8] E. Patelli and H. J. Pradlwarter. “Monte Carlo gradient estimation in high dimensions”. In: *International Journal for Numerical Methods in Engineering* October 2009 (2009), n/a–n/a. ISSN: 00295981. DOI: 10.1002/nme.2687. arXiv: 1010.1724. URL: http://doi.wiley.com/10.1002/nme.2687.

[9] E. Patelli, H. J. Pradlwarter, and G. I. Schuëller. “Global Sensitivity of Structural Variability by Random Sampling”. In: *Computer Physics Communications* 181 (2010), pp. 2072–2081. DOI: 10.1016/j.cpc.2010.08.007.

[10] Edoardo Patelli. *Handbook of Uncertainty Quantification*. 2017. ISBN: 978-3-319-12384-4. DOI: 10.1007/978-3-319-12385-1. arXiv: 1507.00398. URL: http://link.springer.com/10.1007/978-3-319-12385-1.

[11] Edoardo Patelli et al. “OpenCossan 2.0: an efficient computational toolbox for risk, reliability and resilience analysis”. In: *Proceedings of the joint ICVRAM ISUMA UNCERTAINTIES conference*. 2018 (submitted).

[12] M.A. Pick et al. “The new first wall configuration of JET”. In: *15th IEEE/NPSS Symposium. Fusion Engineering*. Vol. 1. IEEE, pp. 27–30. ISBN: 0-7803-1412-3. DOI: 10.1109/FUSION.1993.518274. URL: http://ieeexplore.ieee.org/document/518274/.

[13] Stefano Tarantola, Debora Gatelli, and Thierry A Mara. “Random balance designs for the estimation of first order global sensitivity indices To cite this version : Random Balance Designs for the Estimation of First Order Global Sensitivity Indices”. In: (2014).

[14] R. Wenninger et al. “The DEMO wall load challenge”. In: *Nuclear Fusion* 57.4 (2017), p. 046002. ISSN: 0029-5515. DOI: 10.1088/1741-4326/aa4fb4. URL: http://stacks.iop.org/0029-5515/57/i=4/a=046002?key=crossref.3401e3bb0178287820bd5518eec20822.

RESPONSIBILITY NOTICE

The authors are the only responsible for the printed material included in this paper.